

AD-A037 956

ROME AIR DEVELOPMENT CENTER GRIFFISS AFB N Y  
ELECTRON MICROSCOPE STUDY OF DEFECTS IN ANNEALED BORON IMPLANTE--ETC(U)  
DEC 76 J J COMER, S A ROOSILD  
RADC-TR-76-398

F/G 20/12

UNCLASSIFIED

NL

1 of 1  
ADA037956



END  
DATE  
FILMED  
4-77

ADA 037956

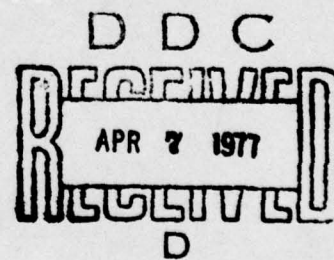
RADC-TR-76-398  
IN-HOUSE REPORT  
DECEMBER 1976



## Electron Microscope Study of Defects in Annealed Boron Implanted Silicon

JOSEPH J. COMER  
SVEN A. ROOSILD

Approved for public release; distribution unlimited.



AD No. \_\_\_\_\_  
DDC FILE COPY

ROME AIR DEVELOPMENT CENTER  
AIR FORCE SYSTEMS COMMAND  
GRIFFISS AIR FORCE BASE, NEW YORK 13441

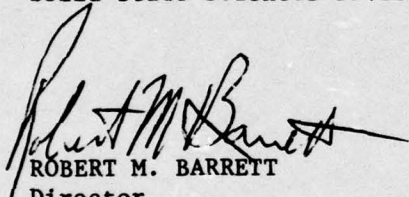
This report has been reviewed by the RADC Information Office (OI) and is releasable to the National Technical Information Service (NTIS).

This report has been reviewed and is approved for publication.

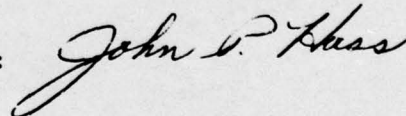
APPROVED:

HAROLD POSEN, Chief  
Materials & Devices Evaluation Branch  
Solid State Sciences Division

APPROVED:

  
ROBERT M. BARRETT  
Director  
Solid State Sciences Division

FOR THE COMMANDER:



*MISSION*  
*of*  
*Rome Air Development Center*

*RADC plans and conducts research, exploratory and advanced development programs in command, control, and communications (C<sup>3</sup>) activities, and in the C<sup>3</sup> areas of information sciences and intelligence. The principal technical mission areas are communications, electromagnetic guidance and control, surveillance of ground and aerospace objects, intelligence data collection and handling, information system technology, ionospheric propagation, solid state sciences, microwave physics and electronic reliability, maintainability and compatibility.*



Printed by  
United States Air Force  
Hanscom AFB, Mass. 01731

Unclassified

SECURITY CLASSIFICATION OF THIS PAGE (When Data Entered)

REPORT DOCUMENTATION PAGE

READ INSTRUCTIONS BEFORE COMPLETING FORM

14) 1. REPORT NUMBER RADC-TR-76-398	2. GOVT ACCESSION NO.	3. RECIPIENT'S CATALOG NUMBER (9)
6) TITLE (and Subtitle) ELECTRON MICROSCOPE STUDY OF DEFECTS IN ANNEALED BORON IMPLANTED SILICON.		5. TYPE OF REPORT & PERIOD COVERED Scientific. - Interim / rept.)
10) AUTHOR(S) Joseph J. Comer Sven A. Roosild		6. PERFORMING ORG. REPORT NUMBER 17
9. PERFORMING ORGANIZATION NAME AND ADDRESS Deputy for Electronic Technology (RADC/ETSO) Hanscom AFB Massachusetts 01731		8. CONTRACT OR GRANT NUMBER(S)
11. CONTROLLING OFFICE NAME AND ADDRESS Deputy for Electronic Technology (RADC/ETSO) Hanscom AFB Massachusetts 01731		10. PROGRAM ELEMENT PROJECT, TASK AREA & WORK UNIT NUMBERS 61102F 2306J103
14. MONITORING AGENCY NAME & ADDRESS (if different from Controlling Office)		12. REPORT DATE 11) December 1976
12) 24p.		13. NUMBER OF PAGES 24
16) 2306		15. SECURITY CLASS. (of this report) Unclassified
17) 51		15a. DECLASSIFICATION/DOWNGRADING SCHEDULE
16) 2306   17) 51 16. DISTRIBUTION STATEMENT (of this Report) Approved for public release; distribution unlimited.		
17. DISTRIBUTION STATEMENT (of the abstract entered in Block 20, if different from Report)		
18. SUPPLEMENTARY NOTES		
19. KEY WORDS (Continue on reverse side if necessary and identify by block number) Silicon devices Boron implantation Annealing Characterization of defects		
20. ABSTRACT (Continue on reverse side if necessary and identify by block number) → Transmission electron microscopy was used to characterize defects observed in silicon, following boron implantation through an oxide film and annealing in nitrogen or argon to 950°C.  Rod defects, believed by some to be boron precipitates, are formed upon annealing from 600°C to 700°C. Most of these defects disappear upon annealing to 950°C when maximum electrical activity is achieved. At this point, most →		

309050

JB



## Preface

The authors thank Joseph Lorenzo for help in preparing the specimens. We also appreciate the help of Charles Bergeron and Richard Dowling in preparing the specimens for electron microscopy and for careful printing of the electron micrographs.

## Contents

1. INTRODUCTION	7
2. EXPERIMENTAL	8
3. RESULTS	9
3.1 Types of Defects Observed	9
3.2 Description of the Loop Rows	9
3.3 Diffraction Contrast Experiments	12
3.4 Description of Other Defects	14
4. DISCUSSION OF RESULTS	17
5. CONCLUSIONS	21
REFERENCES	23

## Illustrations

1. Dislocation Loops and Dipoles in Boron Implanted Silicon After Annealing to 950°C	10
2. Small Precipitate Particles in Boron Implanted Silicon Annealed to 950°C	10
3. Rod-Shaped Defects in Boron Implanted Silicon After Annealing to 800°C	11
4. Rod-Shaped Defects and Loop Rows in Boron Implanted Silicon Annealed to 950°C	11

## Illustrations

5. Loop Row in Boron Implanted Silicon Showing Increasing Loop Diameters and Spacings Between Loops at Both Ends	12
6. Contrast Behavior of Loop Rows	13
7. Showing Bent Loop Rows	14
8. Region Showing Larger Loops, Single Dislocations and Stacking Faults (Arrows)	15
9. Dipoles Pinching Off Loops	15
10. Partial Dissolution of a Rod Defect	16
11. Precipitate Formation on a Faulted Loop	16

## Electron Microscope Study of Defects in Annealed Boron Implanted Silicon

### 1. INTRODUCTION

The generation of defects in semiconductors such as silicon during device processing, is of serious concern because of the deleterious effect dislocations, precipitates and stacking faults have on the electrical properties of a device. These defects lead to increased leakage currents, thereby affecting lifetime and reliability. Before these defects can be avoided or eliminated, they must be detected at various stages of processing to determine what causes them. One of the most powerful tools for doing this is the transmission electron microscope. This report describes the application of this instrument to the study of defects in boron implanted silicon.

In the fabrication of devices utilizing ion implanted silicon where a passivating dielectric layer is required, the dopant, in this case boron, is often implanted through a thermally-grown oxide film at the surface of the silicon wafer. In this way one avoids a high temperature post-implantation oxidation which would cause some redistribution of the boron atoms by diffusion. However, it is still necessary to anneal the specimen to 950°C to reach maximum electrical activity by causing the boron atoms to move into substitutional positions in the crystal. Bicknell and

---

(Received for publication 5 January 1977)

Allen<sup>1</sup> employing transmission electron microscopy found that the temperature required to reach this condition, coincides with the disappearance of rod-like defects first appearing after a 700°C anneal when boron ions are implanted into bare silicon. These rod-like defects are considered by some to be caused by rows of boron atoms.<sup>1-4</sup>

While studying specimens which had been implanted with boron through an oxide film and then annealed to 950°C, some regions were found to contain rows of small loops, often of the same diameter and equidistant from each other. These loops form as the rod defects disappear. This report describes these loop rows and shows how they are related to the rod defects observed at lower temperatures. It also describes other defects believed to be related to the rod defects.

## 2. EXPERIMENTAL

The silicon specimens were in the form of (111) oriented n-type wafers of 10-mils thickness, having a resistivity of 90 to 100 Ωcm. A 2000Å thick oxide film was grown on the chemically polished surface using steam at 950°C for 30 min. Boron was implanted through the oxide at 180 keV to a dose of  $10^{15}$  B<sup>+</sup>/cm<sup>2</sup>. After implantation, specimens were annealed in nitrogen at 950°C for 1/2 hr. The oxide layer was removed in 1:1 HF-H<sub>2</sub>O and specimen discs 3 mm in diameter were cut ultrasonically and thinned for transmission electron microscopy by jet chemical etching. Specimens were examined in a JEM-6A electron microscope containing a tilting attachment limited to angles of ±20°. The microscope was operated at an accelerating voltage of 100 kV.

1. Bicknell, R.W., and Allen, R.M. (1970) Correlation of electron microscope studies with the electrical properties of boron implanted silicon, Rad. Effects 6:45-49.
2. Davidson, S.M., and Booker, G.R. (1970) Damage produced by ion implantation in silicon, Rad. Effects 6:33-43.
3. Chadderton, L.T., and Eisen, F.H. (1971) On the annealing of damage produced by boron ion implantation of silicon single crystals, Rad. Effects 7:129-138.
4. Wu, Wei-Kuo, and Washburn, J. (1975) Boron precipitates in ion implanted silicon, Proc. 33rd Annual Meeting of the Electron Microscopy Society of America, pp. 256-257.

### 3. RESULTS

#### 3.1 Types of Defects Observed

The various defects observed in these specimens are categorized as follows: (1) *Single dislocation loops or dipoles* are shown in Figure 1; (2) *small rounded precipitate particles* shown in Figure 2; (3) *rod-shaped defects* generally believed to be boron precipitates;<sup>1-4</sup> and (4) *rows of closely-spaced loops*. The rod-shaped defects first appearing at about 700°C are shown in Figure 3 in a specimen annealed to 800°C where they are aligned along  $\langle 110 \rangle$  or  $\langle 112 \rangle$  directions. Figure 4 illustrates that after annealing to 950°C some rod defects are still present, but the main defects are loops, both rows of circular ones or of dipoles. Some workers have observed the dipoles to form from the rod defects upon annealing to this temperature.<sup>3</sup> As with the rods, many of the dipoles also lie along  $\langle 110 \rangle$  or  $\langle 112 \rangle$  directions. Both elongated and circular loops occurring in rows lie on  $\{111\}$  planes. The rounded precipitate particles seen in Figure 2 are usually associated with the dipoles or other loops. These particles are not to be confused with copper silicide particles which have been found in colonies in similar samples when cooled rapidly from 950°C.<sup>5</sup> The identity of the precipitates in the present study has not been established.

#### 3.2 Description of the Loop Rows

The lengths of the loop rows varied from about 0.5  $\mu\text{m}$  to 2  $\mu\text{m}$  or within the size range observed for the rod-shaped defects. Stereo electron microscopy showed that the rows vary in depth in the section under examination, with none found closer than  $\sim 2500\text{\AA}$  to the surface. The remarkable uniformity in diameters and spacing of the loops in some rows is seen in Figure 4. But in other rows the diameters of the loops at each end becomes greater than those in the middle, and as this occurs there is a corresponding increase in separation from the nearest neighbor. This tapering effect is seen in a highly enlarged image of a row in Figure 5. This indicates that the diameter of the loops is limited by the stress imposed by its nearest neighbors.

---

5. Comer, J.J., and Roosild, S.A. (1976) Transmission Electron Microscope Study of Oxidation-Induced Precipitate Defects in Boron-Implanted Silicon, Presented at Electronic Materials Conf., Salt Lake City, Utah, June 23-25, 1976. Submitted to J. Electronic Materials.

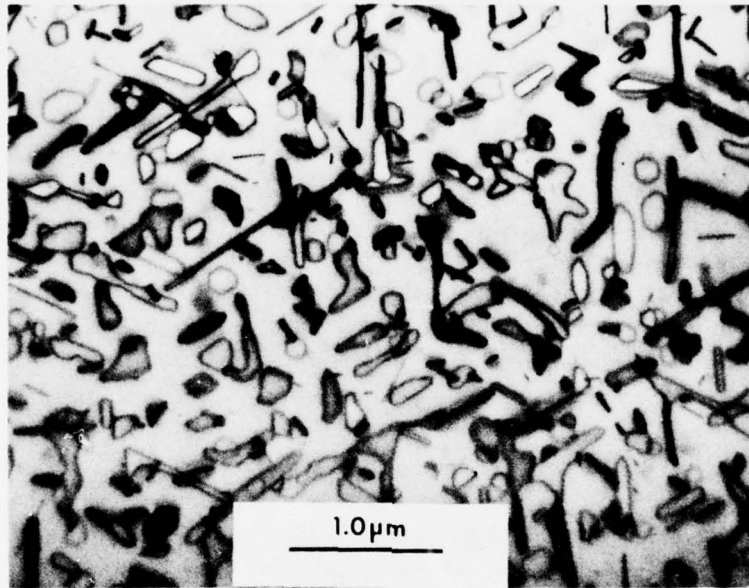


Figure 1. Dislocation Loops and Dipoles in Boron Implanted Silicon After Annealing to 950°C

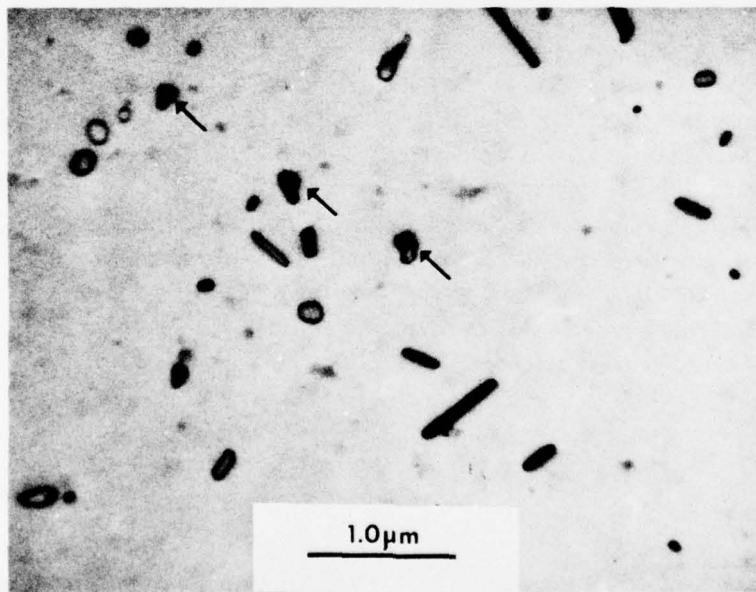


Figure 2. Small Precipitate Particles Arrows in Boron Implanted Silicon Annealed to 950°C

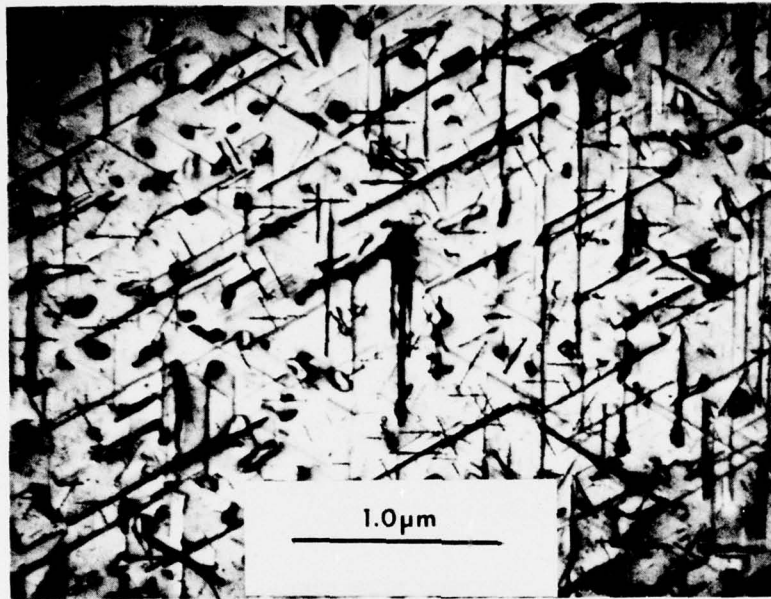


Figure 3. Rod-Shaped Defects in Boron Implanted Silicon After Annealing to 800°C

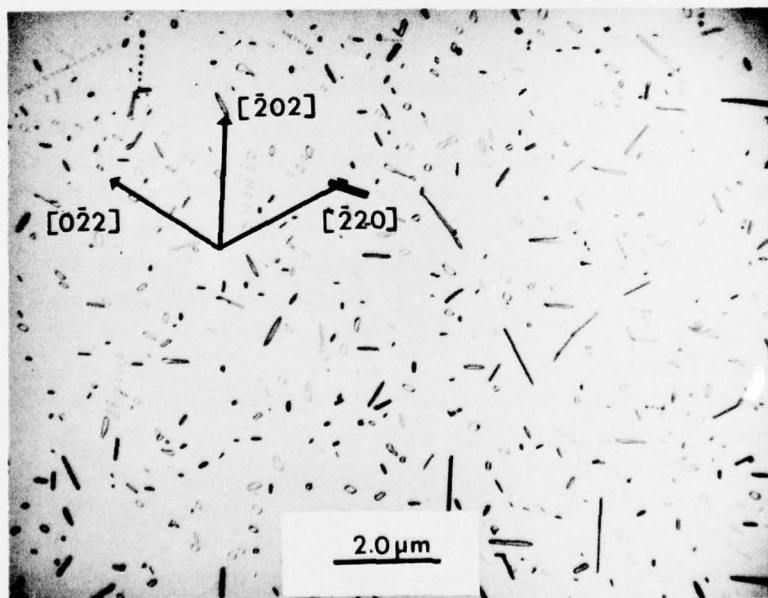


Figure 4. Rod-Shaped Defects and Loop Rows in Boron Implanted Silicon Annealed to 950°C

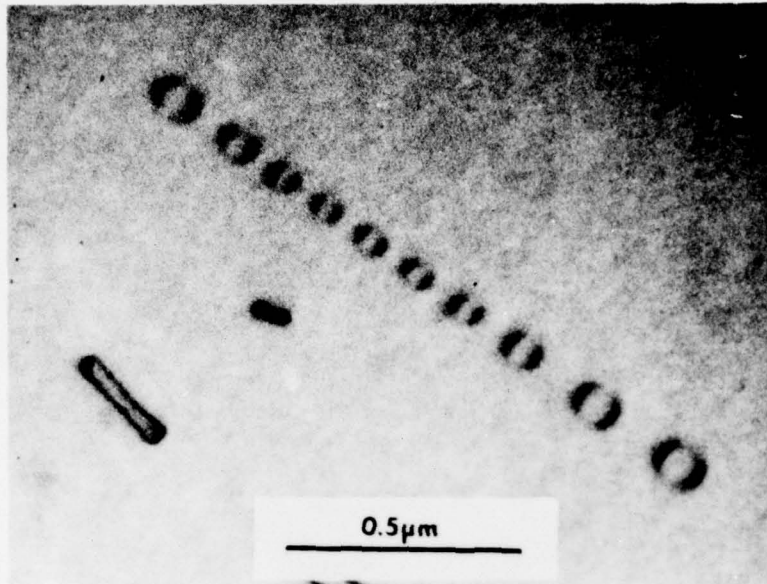


Figure 5. Loop Row in Boron Implanted Silicon Showing Increasing Loop Diameters and Spacings Between Loops at Both Ends

### 3.3 Diffraction Contrast Experiments

When the specimen was tilted to observe the loops under different diffraction conditions by changing the operating  $\bar{g}$  vector, those rows of loops parallel to  $\bar{g}$  either went out of contrast or exhibited minimum contrast, whereas for all other  $\bar{g}$  vectors they remained in strong contrast. This behavior is similar to that observed for the rod defects and is illustrated in Figures 6a and 6b which shows types of defects. In Figure 6a with  $\bar{g}$  parallel to loop row A, only a faint residual contrast is seen whereas rods B and C are in strong contrast. In Figure 6b with the  $\bar{g}$  vector parallel to rods B and C, they reach minimum contrast and loop row A is in strong contrast.

Some loop rows change from one  $\langle 110 \rangle$  direction to another to form an angle of  $120^\circ$  between the segments, each of which contains approximately the same number of loops. This phenomenon is shown in Figure 7 where row AB lies along the  $[\bar{2}02]$  direction and BC along the  $[1\bar{1}\bar{1}]$  direction. Obviously, the loops must lie on different  $\{111\}$  planes and this is indicated by stereo micrographs of some bent loop rows which show a separation in depth below the surface for the two

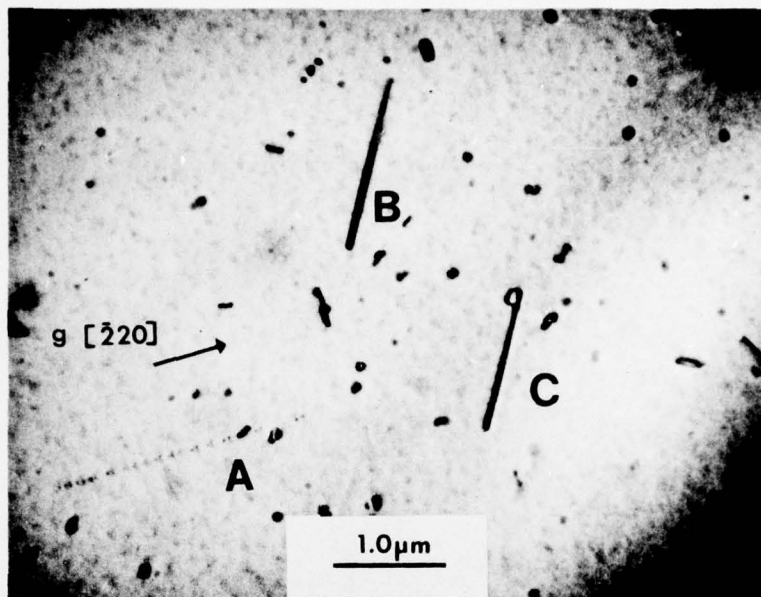


Figure 6a. Contrast Behavior of Loop Rows. With  $\bar{g} = [\bar{2}20]$  parallel to loop row A, only a faint residual contrast is seen. Rod Defects B and C are in Strong Contrast

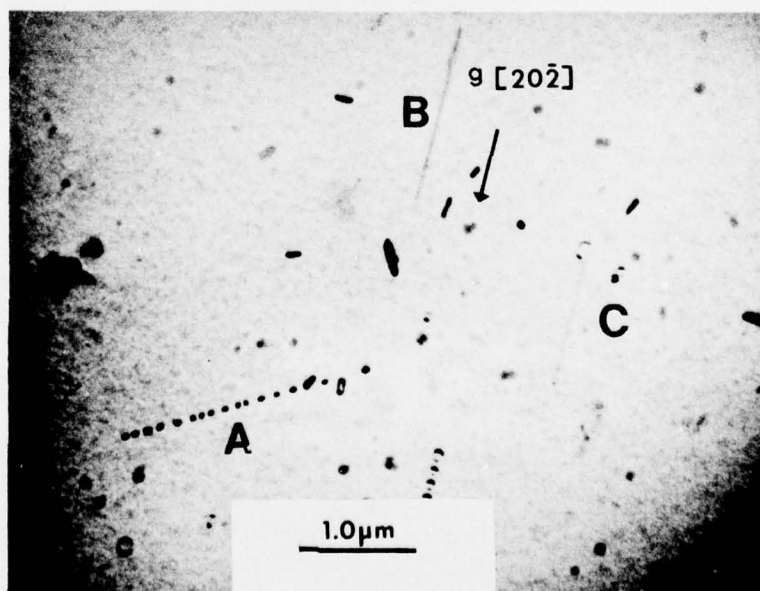


Figure 6b. Contrast Behavior of Loop Rows. With  $\bar{g} = [20\bar{2}]$  parallel to rods B and C, they are at minimum contrast. Loop row A is now in strong contrast

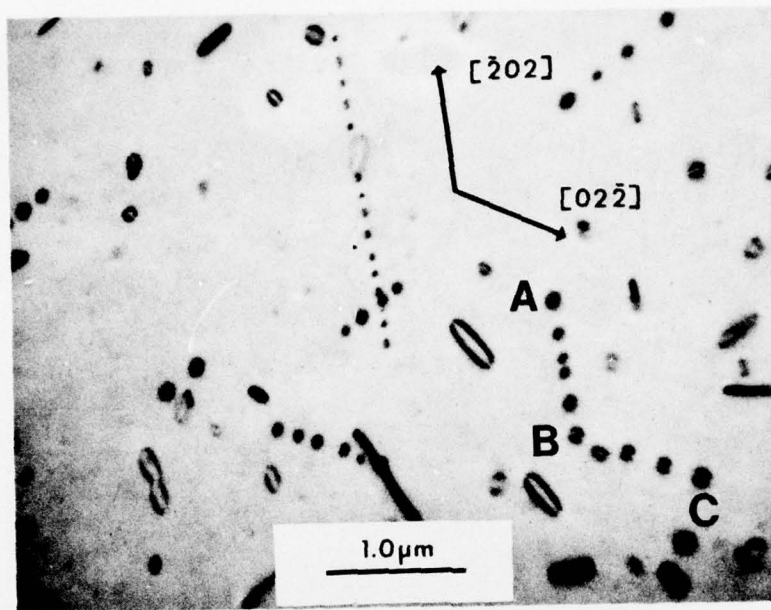


Figure 7. Showing Bent Loop Rows. Note segment AB lies along  $[202]$  and BC along the  $[022]$  direction

segments. It was not possible to analyze the loops in the rows but those single loops lying on  $\{111\}$  planes were mainly prismatic, with Burgers vectors of

$$b = \frac{a}{2} [110] \quad .$$

### 3.1 Description of Other Defects

Not all regions contain rows of loops. In fact, most of the specimen resembles the area shown in Figure 8 containing larger loops, single dislocations, and some small stacking faults. Another region shown in Figure 9 shows dipoles pinching off loops at A, B, and C. Strain contrast within the dipole D suggests partial dissolution of one of the rod defects. A similar feature is seen in Figure 10. This same micrograph shows black spots believed to represent strain fields around precipitate particles similar to those shown earlier in Figure 2. Another example of precipitate formation, on a faulted loop, is seen in Figure 11.

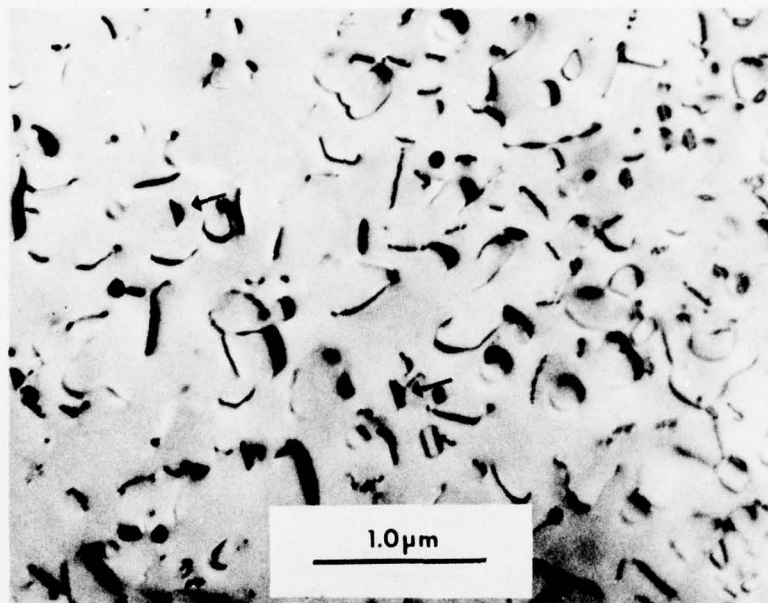


Figure 8. Region Showing Larger Loops, Single Dislocations and Stacking Faults (Arrows)

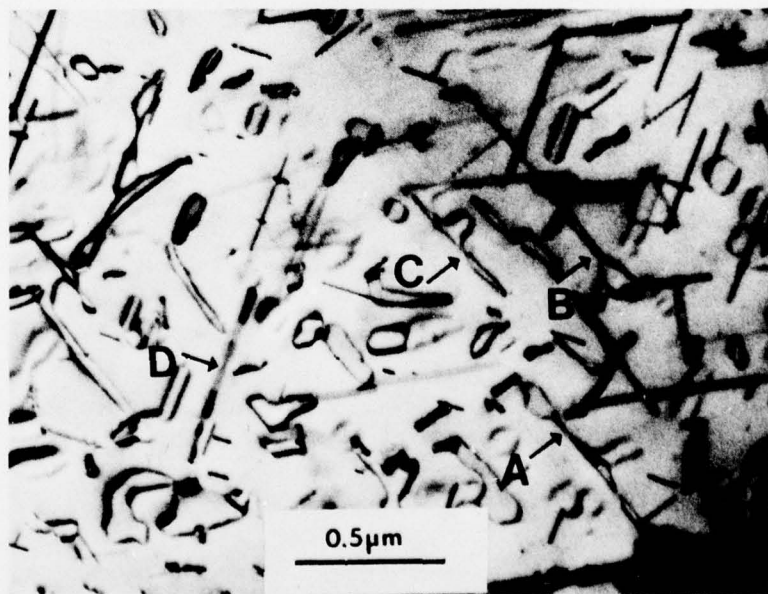


Figure 9. Dipoles Pinching Off Loops. See A, B, and C. Note the unusual strain contrast at D

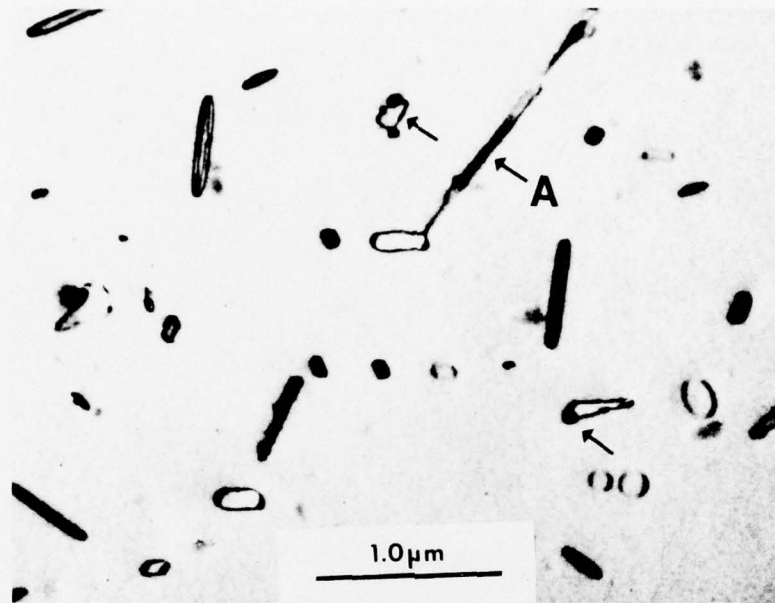


Figure 10. Partial Dissolution of a Rod Defect. See arrow (A). Other arrows show precipitate particles

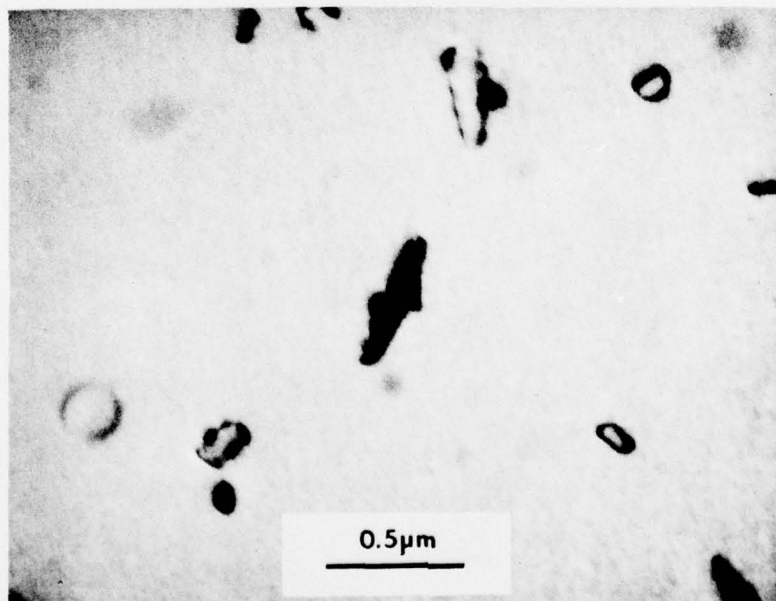


Figure 11. Precipitate Formation on a Faulted Loop

#### 4. DISCUSSION OF RESULTS

Two possible mechanisms for the formation of the loop rows must be considered: (1) The loops are generated to relieve stress set up around a defect in the crystal which may be an artificially introduced inclusion or particle of a precipitated second phase;<sup>6</sup> or (2) the loops form by break-up of a dipole to lower its elastic energy.

Many examples of the first type of loop formation are found in the literature for various materials including silicon.<sup>7, 8</sup> In each case the generation of prismatic loops was initiated by differential expansion, or volume change of a precipitate, or inclusion due to rapid cooling of the specimen, and it has been suggested that they form by degeneration of dislocation helices.<sup>6</sup>

In a theoretical treatment dealing with the spacings of these loops, Bullough and Newman<sup>9</sup> derived the stresses and displacement associated with a single circular edge prismatic loop of strength  $b$  and radius  $r$  on a cylindrical glide surface. They showed how the shear stress  $\text{Prz}$  around a single loop decreases rapidly with distance  $z$  from the loop. According to their interpretation, when a loop is generated at a precipitate it glides on the glide cylinder surface under axial stress and causes the other loops in the row to move further away until a final equilibrium configuration is attained. At this point, the shear stress on each loop due to its neighbors is equal to the critical shear stress required to move the loop. The critical shear stress is given as

$$\text{Prz crit.} = Vb\mu/4\pi a(1 - \nu)$$

where  $\mu$  is the shear modulus,  $\nu$  Poisson's ratio,  $a$  the loop radius, and  $V$  a dimensionless parameter which is a function of the loop radius.

Regarding the second method of loop formation, which involves the break-up of dipoles to lower their elastic energy, both Bicknell and Allen,<sup>1</sup> and Chadderton and Eisen<sup>3</sup> observed the transformation of rod defects into circular loops upon annealing boron implanted silicon, but there was no report of loop rows of the type under discussion here. In the present study, many examples of dipoles pinching off into loops were found as illustrated earlier in Figure 9. Most of these evolved

6. Jones, D.A., and Mitchell, J.W. (1958) Observations of helical dislocations in silver chloride, *Phil. Mag.* 3:1- .
7. Barnes, R.S., and Mazey, D.J. (1963) Stress-generated prismatic dislocation loops in quenched copper, *Acta. Met.* 11:281-286.
8. Dash, William C. (1958) Generation of prismatic dislocation loops in silicon, *Phys. Rev. Letters* 1:400-402.
9. Bullough, R., and Newman, R.C. (1960) The spacing of prismatic dislocation loops, *Phil. Mag.* 5:921-927.

into irregularly shaped loops of various sizes and numbers of no apparent relationship to the rod defects. It appears that the evolution of the loop rows reported in this study is a unique occurrence representing almost a spontaneous generation of loops from the rod defects. This is suggested by the similarity in lengths of loop rows and rods as well as their diameters.

Obviously, the identity of the rod-like defects is basic to understanding the annealing characteristics of boron-implanted silicon within the temperature range under discussion. There is no ready analytical technique which can be applied to solve this problem. Attempts by workers to obtain selected area diffraction patterns have been unsuccessful, and because of its low atomic number boron cannot be identified in transmission electron microscopes using energy dispersive techniques. Therefore, at the present time, one can only speculate as to the identity of the rod defects on the basis of indirect evidence obtained by transmission electron microscopy coupled with electrical measurements.

The rod-shaped defects have been observed over a range of temperatures from 600 to 900°C with some persisting to 950°C or more. They are out of contrast only when  $\bar{g}$ , the reciprocal lattice vector of the diffracted beam used in image formation, is parallel to the long direction of the rod. This indicates a cylindrically symmetric strain field, suggesting to various workers that the rods are boron precipitates, rows of interstitials, vacancies, or some other form of impurity. The disappearance of most of the rods, coinciding with the attainment of maximum electrical activity, indicates that most of the boron atoms have gone into substitutional positions and further supports the view that these defects contain boron.

Recently, Wu and Washburn<sup>4</sup> in studies of boron, implanted silicon annealed in the electron microscope and applied annealing kinetics to identify the defects in question. On holding the specimen at 800°C, they observed differences in the rate of shrinkage of the rods. For one type they derived an activation energy of  $3.5 \pm 0.1$  eV and concluded that the rate controlling process was boron diffusion, leading to the conclusion that at least one type of rod defect is composed of boron atoms. Their observation that some rods rotate off the  $\langle 110 \rangle$  direction to a  $\langle 112 \rangle$  direction is in agreement with our observation of bent loop rows. Although we observed bending from one  $\langle 110 \rangle$  direction to another, the results support our view that the loop rows are derived from dissolution of the rods where the loop rows maintain the original positions of the rods.

While most of the results obtained in this study are merely in agreement with results reported earlier by others, we feel that the new evidence of loop rows supports the idea that the rod defects are composed of rows of boron atoms. In summarizing the events that occur upon annealing, it is observed that some rod

defects may rotate and align themselves along different crystallographic directions upon heating from 600°C through 950°C; some will shrink without leaving a trace or else leave an elongated dipole or loop row reflecting the behavior of the rods. In a few examples, we have found possible evidence of a transitional state between rod and dipole as shown in Figures 10 and 11 where the contrast suggests partial dissolution of a rod defect over part of its length rather than by shrinkage.

The break-up of a dipole to lower its elastic energy is seen in several micrographs in this report. Although it is not known why dipole or loop formation is not always seen following the disappearance of a rod defect, it is not unusual for these defects to form to minimize stress in the region. The formation of rows of loops described in this report is not a common occurrence, yet it appears from the evidence presented that they evolve from the dissolution or break-up of the rod defects. The loop rows closely resemble those produced by prismatic pinching; for example, the envelope of the loop tapers on either side of the row center as the loop diameter and spacing between loops increase simultaneously to maintain equilibrium.<sup>7-9</sup> In effect, as end members of the rows are repelled by their neighbors, they are free to increase their diameter by climb. This was illustrated in Figure 5. Yet, despite the resemblance to loop rows formed by prismatic pinching, there is no other evidence to support the idea of this type of loop generation. However, as there is evidence of dipole formation following dissolution of the rod defects, it seems likely that the loop rows result from the break-up of the elongated loops. But the unusual contrast behavior of the loop rows has still not been explained. The rows behave as though they were part of a single edge dislocation at maximum contrast with  $\bar{g}$  normal to the long direction. This suggests that the loops have a strain vector normal to the loop plane. This could occur if the loops actually enclosed thin discs of impurities having their displacement vector normal to the plane of the disc. In the case of those loops which have been determined to be interstitial, climb occurs by absorption of interstitial atoms. Since electrical measurements at this stage indicate that most of the boron atoms are in substitutional positions, it is concluded that the loops contain silicon atoms as proposed by others.<sup>10</sup>

The Watkins mechanism<sup>11</sup> has been proposed by Bicknell and Allen<sup>1</sup> as a possible explanation of how the rod defects form. By this mechanism, interstitial silicon atoms produced by implantation damage eject substitutional boron atoms

---

10. Bicknell, R.W. (1969) The distribution of condensed defect structures formed in annealed boron-implanted silicon, *Proc. Roy. Soc. A* 311:75-78.

11. Watkins, G.D. (1964) A review of EPR studies in irradiated silicon radiation damage in semiconductors, *7th Inter. Conf. on the Physics of Semiconductors*, Academic Press, pp. 97-111.

upon annealing to about 700°C. This is accompanied by clustering and precipitation of boron atoms while the silicon goes into substitutional positions. The same mechanism was recently proposed by Hofker<sup>12</sup> as a result of studies made of the redistribution of boron by secondary ion mass spectrometry.

Assuming that this mechanism is reversible, the following explanation for the rod defects is offered. These defects consisting of rows of interstitial boron atoms are no longer stable at temperatures of 700°C or higher and move into substitutional positions to replace silicon atoms. The dipoles and loops result from a coalescence of these interstitial silicon atoms. Actually, this idea had been proposed by Bicknell several years ago.<sup>10</sup> The presence of small precipitate particles at dislocation sites at 950°C or above is believed related to the formation of a small amount of silicon boride. It is quite possible to form compounds such as SiB<sub>4</sub> or SiB<sub>6</sub> at temperatures above 900°C. Arai, Nakamura and Terunuma<sup>13</sup> have presented electron diffraction evidence of such compound formation at the interface of B<sub>2</sub>O<sub>3</sub> and silicon within the temperature range 900°C-1200°C. Also, the present authors have identified by selected area electron diffraction single crystal precipitates of SiB<sub>6</sub> following a 1250°C anneal of boron implanted silicon.<sup>14</sup> The presence of precipitates following anneals up to 900°C has not been reported by others. However, they are not unique to specimens implanted through an oxide film and have been observed upon implantation in bare silicon followed by annealing to 1100°C.<sup>14</sup>

There are many questions remaining to be answered. For example, it is not known why some rod defects simply shrink and disappear without trace, or why some rods bend along different planes. From observations of the bent loop rows, which are assumed to form from bent rod defects, it appears that bending is due to transference of material to a different plane in a different crystallographic direction. The resulting segments of loop rows lie on different {111} planes. The formation of the loop rows represent a stage in the dissolution of the rod defects which may be seen only under certain conditions of specimen annealing or cooling.

12. Hofker, W.K. (1975) Implantation of boron in silicon, Philips Res. Report, Suppl. 8:1-7.
13. Arai, E., Nakamura, H., and Terunuma, G. (1973) Interface reactions of B<sub>2</sub>O<sub>3</sub>-Si system and boron diffusion into silicon, J. Electrochem. Soc. 120:980-987.
14. Comer, J.J., and Roosild, S.A. (1975) Electron microscope observations of precipitation in boron implanted silicon, Rad. Effects 25:275-277.

## 5. CONCLUSIONS

The results reported here support the view that boron atoms coalesce to form the rod defects observed on annealing boron implanted silicon to 700°C. At higher temperatures the defects become unstable and eventually most of the boron atoms move into substitutional positions. Associated with this dissolution is the formation of dipoles and loops resulting from the coalescence of silicon atoms which are displaced into interstitial positions. A small number of boron atoms interact with silicon to form small particles, possibly a silicon boride, occurring mainly at the sites of dislocations. The loop rows, seen infrequently, are generated by the break-up of the rod defects. The end loops grow by climb, increasing their diameters and separation from their neighbors, and eventually breaking free of the attractive forces holding them to the row.

## References

1. Bicknell, R.W., and Allen, R.M. (1970) Correlation of electron microscope studies with the electrical properties of boron implanted silicon, Rad. Effects 6:45-49.
2. Davidson, S.M., and Booker, G.R. (1970) Damage produced by ion implantation in silicon, Rad. Effects 6:33-43.
3. Chadderton, L.T., and Eisen, F.H. (1971) On the annealing of damage produced by boron ion implantation of silicon single crystals, Rad. Effects 7:129-138.
4. Wu, Wei-Kuo, and Washburn, J. (1975) Boron precipitates in ion implanted silicon, Proc. 33rd Annual Meeting of the Electron Microscopy Society of America, pp 256-257.
5. Comer, J.J., and Roosild, S.A. (1976) Transmission Electron Microscope Study of Oxidation-Induced Precipitate Defects in Boron-Implanted Silicon, Presented at Electronic Materials Conf., Salt Lake City, Utah, June 23-25, 1976. Submitted to J. Electronic Materials.
6. Jones, D.A., and Mitchell, J.W. (1958) Observations of helical dislocations in silver chloride, Phil. Mag. 3:1- .
7. Barnes, R.S., and Mazey, D.J. (1963) Stress-generated prismatic dislocation loops in quenched copper, Acta. Met. 11:281-286.
8. Dash, William C. (1958) Generation of prismatic dislocation loops in silicon, Phys. Rev. Letters 1:400-402.
9. Bullough, R., and Newman, R.C. (1960) The spacing of prismatic dislocation loops, Phil. Mag. 5:921-927.
10. Bicknell, R.W. (1969) The distribution of condensed defect structures formed in annealed boron-implanted silicon, Proc. Roy. Soc. A 311:75-78.
11. Watkins, G.D. (1964) A review of EPR studies in irradiated silicon radiation damage in semiconductors, 7th Inter. Conf. on the Physics of Semiconductors, Academic Press, pp. 97-111.

12. Hofker, W.K. (1975) Implantation of boron in silicon, Philips Res. Report. Suppl. 8:1-7.
13. Arai, E., Nakamura, H., and Terunuma, G. (1973) Interface reactions of  $B_2O_3$ -Si system and boron diffusion into silicon, J. Electrochem. Soc. 120:980-987.
14. Comer, J.J., and Roosild, S.A. (1975) Electron microscope observations of precipitation in boron implanted silicon, Rad. Effects 25:275-277.